

# AIP | Applied Physics Letters

## Remote doping of a pentacene transistor: Control of charge transfer by molecular-level engineering

Wei Zhao, Yabing Qi, Tissa Sajoto, Stephen Barlow, Seth R. Marder et al.

Citation: *Appl. Phys. Lett.* **97**, 123305 (2010); doi: 10.1063/1.3491429

View online: <http://dx.doi.org/10.1063/1.3491429>

View Table of Contents: <http://apl.aip.org/resource/1/APPLAB/v97/i12>

Published by the [American Institute of Physics](http://www.aip.org).

### Additional information on *Appl. Phys. Lett.*

Journal Homepage: <http://apl.aip.org/>

Journal Information: [http://apl.aip.org/about/about\\_the\\_journal](http://apl.aip.org/about/about_the_journal)

Top downloads: [http://apl.aip.org/features/most\\_downloaded](http://apl.aip.org/features/most_downloaded)

Information for Authors: <http://apl.aip.org/authors>

## ADVERTISEMENT

**minus k<sup>®</sup> TECHNOLOGY** *20 years* **Improve your Images with Minus K's Negative-Stiffness Vibration Isolation**

**Workstations & Optical Tables** **Bench Top Isolators** **Without Minus K** **With Minus K** **Floor Platforms**

**Custom Applications** **Multi Isolator Systems**



The advertisement features several images of Minus K products: workstations and optical tables, bench top isolators, multi isolator systems, and floor platforms. Two topography images are shown side-by-side, labeled 'Without Minus K' and 'With Minus K'. The 'Without Minus K' image shows a highly textured, noisy surface, while the 'With Minus K' image shows a much smoother surface. The logos for NASA, ESA, JPL, and JWST are displayed under the 'Custom Applications' section.

## Remote doping of a pentacene transistor: Control of charge transfer by molecular-level engineering

Wei Zhao,<sup>1</sup> Yabing Qi,<sup>1</sup> Tissa Sajoto,<sup>2</sup> Stephen Barlow,<sup>2</sup> Seth R. Marder,<sup>2</sup> and Antoine Kahn<sup>1,a)</sup>

<sup>1</sup>Department of Electrical Engineering, Princeton University, Princeton, New Jersey 08544, USA

<sup>2</sup>School of Chemistry and Biochemistry and Center for Organic Photonics and Electronics, Georgia Institute of Technology, Atlanta, Georgia 30332, USA

(Received 14 June 2010; accepted 28 August 2010; published online 22 September 2010)

We demonstrate that holes from a p-doped *N,N'*-diphenyl-*N,N'*-bis(1-naphthyl)-1,1'-biphenyl-4,4'-diamine ( $\alpha$ -NPD) layer transfer to an adjacent pentacene film. The spatial separation of carriers from dopants, or remote doping, is demonstrated with a combination of photoemission spectroscopy and current-voltage measurements for a p-doped  $\alpha$ -NPD/pentacene heterojunction. Increased conductivity of the pentacene film is observed in both nongated temperature-dependent conductivity and gated thin-film transistor measurements. © 2010 American Institute of Physics. [doi:10.1063/1.3491429]

Chemical doping is an effective technique to improve the performance of organic devices.<sup>1–7</sup> Reduced contact resistance, increased film conductivity, and manipulation of interface molecular-level alignment are recognized benefits of doping molecular materials. Powerful n- and p-type molecular dopants have been investigated in the past decade. Among these, the three-dimensional, strong electron-acceptor molybdenum tris[1,2-bis(trifluoromethyl)ethane-1,2-dithiolene] ( $\text{Mo}(\text{tfd})_3$ )<sup>7</sup> (electron affinity EA=5.6 eV) was found highly stable with respect to diffusion in various organic matrices.<sup>8</sup> This stability allows spatial confinement of dopants to specific regions, i.e., within few nanometers of an interface, without subsequent degradation of the device due to dopant diffusion. Reduction of contact resistance in organic field-effect transistors (OFET) has been recently demonstrated in that manner.<sup>9</sup>

One of the effects of doping is to increase charge-carrier mobility by preferentially filling deep traps in the gap of the organic semiconductor, thereby reducing the activation energy for the hopping transport process of the injected carriers.<sup>3,8,10</sup> However, ionized dopants may also lead to disruption of the matrix, or to trapping or scattering of carriers. These effects are less well established, and presumably depend on the nature of the organic thin film (crystalline versus polycrystalline or amorphous). The concept developed in this paper is “remote” doping for organic structures, i.e., the transfer of donated holes or electrons to an active region spatially separated from the region occupied by the dopant molecules. Remote doping, which makes use of energy band engineering to spatially separate carriers from dopants, effectively reduces carrier scattering by ionized dopants and has been found to enhance mobility in inorganic semiconductor systems.<sup>11</sup> Furthermore, the application of direct doping in OFETs often results in difficulties in controlling the charge density in the doped channel with the gate voltage.<sup>12–14</sup> Remote doping with the proper choice of organic heterojunctions in contact with the channel of an OFET offers a potential route to address this issue.

The work presented here is grounded in our understanding of energy-level alignment and charge transfer at doped organic-organic heterojunctions.<sup>15</sup> *N,N'*-diphenyl-*N,N'*-bis(1-naphthyl)-1,1'-biphenyl-4,4'-diamine ( $\alpha$ -NPD) doped with  $\text{Mo}(\text{tfd})_3$  (p-doped  $\alpha$ -NPD) is chosen to transfer holes to the pentacene channel of an OFET. The energy level alignment between the two organic semiconductors, and the charge transfer at the p-doped  $\alpha$ -NPD/pentacene heterojunction, are investigated via ultraviolet photoemission spectroscopy (UPS). Increased conductivity in the remotely doped pentacene film is demonstrated by temperature-dependent conductivity measurement in the nongated configuration. An interlayer placed between p-doped  $\alpha$ -NPD and pentacene, composed of intrinsic  $\alpha$ -NPD or bis(2-(4,6-difluorophenyl)pyridinato-*N,C*<sup>2'</sup>)(picolinato-*N,O*)iridium(III) (Firpic), is shown to hinder the charge transfer between the two layers. We demonstrate that the channel current in the remotely doped pentacene transistor with the interlayer can be modulated by the gate voltage.

In the first experiment, a 60 Å p-doped  $\alpha$ -NPD film is prepared by coevaporation of  $\alpha$ -NPD (H. W. Sands, sublimed grade) with 1%  $\text{Mo}(\text{tfd})_3$  (synthesized and purified as described in the literature<sup>16</sup>) in ultrahigh vacuum (UHV), at 1 Å/s on a gold substrate. The UPS spectrum of the film [bottom curve of Fig. 1(a)] shows the edge of the highest occupied molecular orbital (HOMO) feature at 0.37 eV below the Fermi level,  $E_F$  ( $E_F$  is measured independently on a clean surface of gold). This is ~0.6 eV closer to  $E_F$  than in intrinsic  $\alpha$ -NPD deposited on gold,<sup>7,17</sup> indicative of p-doping and in excellent agreement with previous measurements on  $\alpha$ -NPD: $\text{Mo}(\text{tfd})_3$ .<sup>7</sup> The deposition of 10 Å of pentacene on p-doped  $\alpha$ -NPD (second curve from the bottom) shifts the onset of photoemission toward higher binding energy [left panel, Fig. 1(a)], indicating a decrease in work function due to a positive charge transfer from  $\alpha$ -NPD to pentacene. This is due to the fact that the pentacene ionization energy (IE=5.0 eV) is essentially equal to the work function of p-doped  $\alpha$ -NPD. The system reaches thermal equilibrium by transferring charges to lower the pentacene HOMO below  $E_F$ , in full agreement with previous observations on doped heterojunctions, e.g., n-doped copper phthalocyanine/ $\text{C}_{60}$ .<sup>15</sup>

<sup>a)</sup>Author to whom correspondence should be addressed. Electronic mail: kahn@princeton.edu.

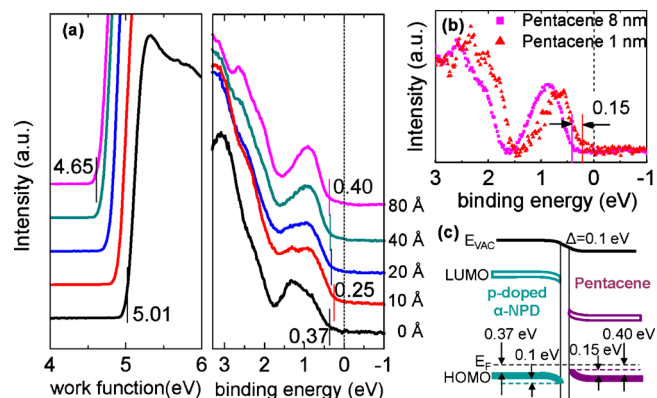


FIG. 1. (Color online) (a) UPS spectra of pentacene incrementally deposited on 1% p-doped  $\alpha$ -NPD. Vertical bars indicate the work function (left panel) and the HOMO edge (right panel). The Fermi level ( $E_F$ ) is the reference 0 eV energy. (b) Pentacene HOMO shift between 10 and 80 Å. (c) Energy level diagram of the 1% p-doped  $\alpha$ -NPD/pentacene heterojunction based on (a) and (b).

The relative  $\alpha$ -NPD and pentacene HOMO positions for various pentacene thicknesses are obtained by decomposition of their respective contributions to the UPS spectra [right panel, Fig. 1(a)]. The results show: (i) a 0.15 eV shift in the pentacene HOMO toward higher binding energy from 10 to 80 Å [Fig. 1(b)]; (ii) a 0.1 eV displacement of the  $\alpha$ -NPD HOMO (not shown here), consistent with positive charge transfer from p-doped  $\alpha$ -NPD to interface pentacene molecules; (iii) a  $\sim 0.2$  eV offset between the pentacene and  $\alpha$ -NPD HOMO edges at the interface [Fig. 1(b)]. The IE of both materials match well previously reported values.<sup>18,19</sup>

The interface charge transfer is further investigated via electrical measurements. Pentacene and  $\alpha$ -NPD or Firpic (Universal Display Corporation) films are grown sequentially in UHV (pentacene always on the bottom) on a quartz substrate prepatterned with interdigitated Ti 20 Å/Au 300 Å electrodes (electrode width: 5 mm; interelectrode gap: 150  $\mu$ m), and transferred for electrical measurement without ambient exposure. Conductivity measurements are performed in the dark on a temperature-controlled stage between 300 and 100 K ( $\Delta T = 10$  K). The current-voltage (I-V) characteristics are recorded with a Keithley source meter 2400. Four devices are investigated: (a) pentacene (400 Å); and pentacene (400 Å)/[interlayer]/p-doped (1%)  $\alpha$ -NPD (400 Å), with [interlayer] consisting of (b) Firpic (100 Å); (c) undoped  $\alpha$ -NPD (100 Å); and (d) no interlayer. Deposition rates for pentacene and p-doped  $\alpha$ -NPD for all devices are 0.2 Å/s and 1.0 Å/s, respectively.

The conductivity ( $\sigma$ ) of these films decreases with temperature following a simple Arrhenius law,  $\sigma \sim \exp[-E_a/(k_B T)]$  (Fig. 2), where  $E_a$  is the activation energy corresponding to a trap and release process for thermally assisted hopping transport.<sup>20</sup> At  $T < 150$  K,  $E_a$  becomes slightly temperature dependent and decreases slowly.  $E_a$  is determined predominantly by the energy distribution of traps and their occupation. Adding the p-doped  $\alpha$ -NPD layer on top of pentacene (d) increases  $\sigma$  from  $4.2 \times 10^{-4}$  to  $1.1 \times 10^{-2}$  S/cm at room temperature as a result of the charge transfer discussed earlier.  $E_a$  decreases from 0.24 to 0.11 eV, suggesting that the charges fill the deeper traps and lower the average energy required for carrier hopping. It is important to clarify that conduction through the p-doped  $\alpha$ -NPD overlayer does not contribute significantly to the overall film

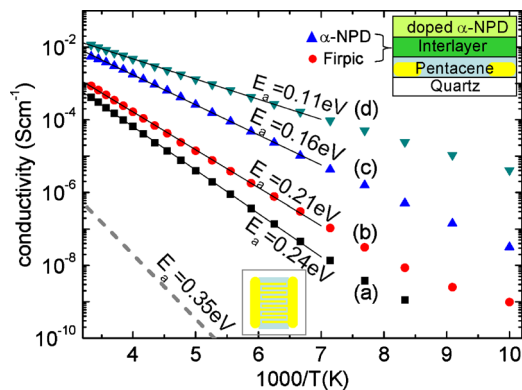


FIG. 2. (Color online) Conductivity ( $\sigma$ ) vs  $T$  for (a) pentacene (400 Å); and pentacene (400 Å)/[interlayer]/p-doped (1%)  $\alpha$ -NPD (400 Å), with an interlayer of: (b) Firpic (100 Å); (c) undoped  $\alpha$ -NPD (100 Å); (d) no interlayer. The dashed line shows  $\sigma$  of a 5000 Å thick 1.7% p-doped  $\alpha$ -NPD film. Full black lines are linear fits to each data set. Insets: top view and cross-section of the nongated device.

ductivity, since  $\sigma$  in an  $\alpha$ -NPD layer, even highly p-doped, is several orders of magnitude lower than in undoped pentacene due to a much lower hole mobility.<sup>12</sup> As evidence, the dashed curve in Fig. 2 represents the  $\sigma(T)$  separately measured for a 5000 Å thick  $\alpha$ -NPD film doped with 1.7% Mo(tfd)<sub>3</sub>.

In devices (b) and (c), a 100 Å interlayer of Firpic or undoped  $\alpha$ -NPD, respectively, is placed between pentacene and p-doped  $\alpha$ -NPD. With the  $\alpha$ -NPD interlayer, the room temperature  $\sigma$  drops by 50% with respect to device (d), which has no interlayer.  $\sigma$  drops significantly more with Firpic (b). Firpic has an IE of 6.0 eV (versus 5.4 for  $\alpha$ -NPD) and has been used in devices as a hole blocking material.<sup>21</sup> The resulting 6.0 eV hole energy barrier between p-doped  $\alpha$ -NPD and pentacene blocks the charge transfer more efficiently than in the case of the  $\alpha$ -NPD interlayer, leading to a significantly lower  $\sigma$  and higher  $E_a$ . Experiments show that, in both cases ( $\alpha$ -NPD or Firpic), the addition of the undoped interlayer alone on the pentacene does not affect the film conductivity and the activation energy. Therefore, the mobility of the pentacene layer does not seem to be affected by the change in the dielectric environment resulting from the addition of the interlayer. Atomic force microscopy measurements on (b) and (c) devices (not shown here) show that  $\alpha$ -NPD and Firpic deposited on pentacene have similar morphology, a result which is important when comparing the behaviors of the two devices. Yet, the interlayer is only 100 Å thick and some leakage due to the roughness of the organic film is to be expected, consistent with the incomplete blocking of the charge transfer in (b).

The increase in the conductivity of the pentacene film is further demonstrated with a gated, top-contact, OFET structure. The substrate is a p<sup>+</sup> Si wafer with a 3000 Å oxide layer (Silicon Quest International). The gate electrode is made by depositing aluminum (5000 Å) at the back of the wafer and annealing in forming gas at 450 °C to form an Ohmic contact. Pentacene (60 Å) followed by doped or undoped  $\alpha$ -NPD films are grown in UHV, and briefly exposed to air (<2 min) before deposition of the gold source and drain contacts (800 Å thick) through a mask. The OFET channel is 100  $\mu$ m long and 2 mm wide. The transistor characteristics (Fig. 3) are measured in nitrogen, using an HP semiconductor analyzer 4155B. The transistor with 300 Å undoped



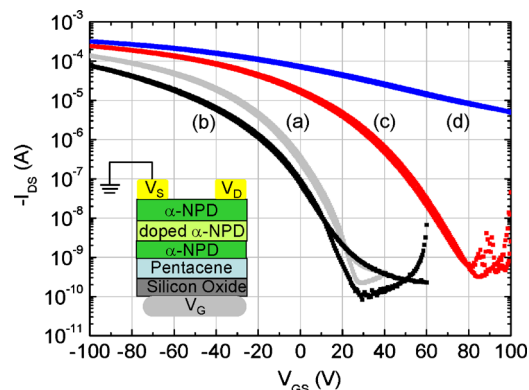


FIG. 3. (Color online) Transfer characteristics at  $V_{DS} = -40$  V of top-contact pentacene OFET. (a) pentacene 300 Å. (b) pentacene 60 Å/ $\alpha$ -NPD 300 Å. (c) pentacene 60 Å/ $\alpha$ -NPD 100 Å/5% p-doped  $\alpha$ -NPD 40 Å/ $\alpha$ -NPD 100 Å. (d) pentacene 60 Å/5% p-doped  $\alpha$ -NPD 40 Å/ $\alpha$ -NPD 200 Å.

$\alpha$ -NPD on top of the 60 Å pentacene layer (b) is used as the reference. The source-drain current  $I_{DS}$  at  $V_{DS} = -40$  V is only slightly smaller than for a simple 300 Å thick pentacene OFET (a). This can be explained since, first, the current in the channel flows mostly in the few layers close to the dielectrics,<sup>22</sup> and, second, Au diffuses through the 300 Å  $\alpha$ -NPD and pentacene layers to make direct contact with the channel.  $\alpha$ -NPD has much poorer hole mobility than pentacene; therefore, it is reasonable to assume that carriers are confined to the thin pentacene layer. In device (d), a 40 Å 5% doped  $\alpha$ -NPD film is deposited on pentacene, followed by a 200 Å undoped  $\alpha$ -NPD film for protection during sample transfer and for keeping the total device thickness approximately constant.  $I_{DS}$  in transistor (d) is almost three orders of magnitude higher than in the undoped pentacene transistors [(a) and (b)] at zero gate voltage ( $V_{GS} = 0$  V). However,  $I_{DS}$  can barely be modulated by the gate bias, in accord with other reports on doped-channel OFETs.<sup>12,13,23</sup> However, when a 100 Å undoped  $\alpha$ -NPD film is placed between pentacene and the doped layer (c), the threshold voltage dramatically decreases and the transistor can be switched off. The  $I_{DS}$  in the presence of the spacer layer is not significantly reduced due to the small charge transfer barrier created by  $\alpha$ -NPD, as seen in the conductivity measurements presented in Figs. 2(c) and 2(d).

The gate field controls both the charge injection from the electrode and charge transfer to the channel from remote doping. However, we assume that the latter is less affected by the gate bias because the threshold voltage in (c) and (d) is increased. Consequently, the field-dependent mobilities can be obtained, to a first approximation, by differentiating the transfer curves in the linear region ( $V_{DS} = -1$  V). The saturated mobility at high operating gate voltage for the remotely doped devices (d) and (c) is  $0.29$   $\text{cm}^2/(\text{V s})$  and  $0.25$   $\text{cm}^2/(\text{V s})$ , respectively, increased from  $0.095$   $\text{cm}^2/(\text{V s})$  for the undoped transistor (b). This is consistent with the decreased activation energy for hole transport, due to the filling of deep traps by remote doping. We recognize that these mobilities, in particular the latter, are at least one order of magnitude lower than standard pentacene OFET mobilities, due to the lack of dielectric surface pretreatment prior to pentacene deposition. The current work is a proof of concept study, and further optimization of the OFETs is currently under way.

The exact function of the undoped interlayer in structure (c), which allows switching off the pentacene channel, is not entirely clear. In remotely doped transistors, carriers are injected from the electrodes as well as from the doped layer. We propose here that the switch-off gate field drives these donated charges from the pentacene to the undoped  $\alpha$ -NPD interlayer, where the mobility is very low and the current does not, therefore, affect the off-current of the transistor. In the absence of this undoped interlayer, emptying the channel by pushing charges back to the doped  $\alpha$ -NPD, where the hole carrier density is already high, is expected to be much more difficult, and switching off the pentacene channel is problematic.

In conclusion, we have investigated the hole transfer from a p-doped  $\alpha$ -NPD film to a pentacene film, which spatially separates the holes from the dopants. Remote doping is confirmed by electrical characterization, both in nongated and gated transistor structures. The amount of charge transfer is found to depend on the energy barrier created by an interlayer. This undoped interlayer plays a critical role in switching off the remotely doped OFET.

Support of this work by the National Science Foundation (Grant No. DMR-1005892), the Princeton MRSEC of the National Science Foundation (Grant No. DMR-0819860), and by Solvay Corporation is gratefully acknowledged. The authors thank Dr. Michael Kröger for help with temperature-dependent conductivity measurements.

- <sup>1</sup>C. Urich, D. Wynands, S. Olthof, M. K. Riede, K. Leo, S. Sonntag, B. Maennig, and M. Pfeiffer, *J. Appl. Phys.* **104**, 043107 (2008).
- <sup>2</sup>X. Zhou, J. Blochwitz, M. Pfeiffer, A. Nollau, T. Fritz, and K. Leo, *Adv. Funct. Mater.* **11**, 310 (2001).
- <sup>3</sup>K. Walzer, B. Maennig, M. Pfeiffer, and K. Leo, *Chem. Rev.* **107**, 1233 (2007).
- <sup>4</sup>C. K. Chan, W. Zhao, A. Kahn, and I. G. Hill, *Appl. Phys. Lett.* **94**, 203306 (2009).
- <sup>5</sup>J. Kido and T. Matsumoto, *Appl. Phys. Lett.* **73**, 2866 (1998).
- <sup>6</sup>C. K. Chan, W. Zhao, S. Barlow, S. Marder, and A. Kahn, *Org. Electron.* **9**, 575 (2008).
- <sup>7</sup>Y. B. Qi, T. Sajoto, S. Barlow, E. G. Kim, J. L. Brédas, S. R. Marder, and A. Kahn, *J. Am. Chem. Soc.* **131**, 12530 (2009).
- <sup>8</sup>Y. B. Qi, T. Sajoto, M. Kroger, A. M. Kandabarow, W. Park, S. Barlow, E. G. Kim, L. Wielunski, L. C. Feldman, R. A. Bartynski, J. L. Brédas, S. R. Marder, and A. Kahn, *Chem. Mater.* **22**, 524 (2010).
- <sup>9</sup>S. P. Tiwari, W. Potscavage, T. Sajoto, S. Barlow, S. R. Marder, and B. Kippelen, *Org. Electron.* **11**, 860 (2010).
- <sup>10</sup>G. Pfister, *Phys. Rev. B* **16**, 3676 (1977).
- <sup>11</sup>P. M. Solomon and H. Morkoc, *IEEE Trans. Electron Devices* **31**, 1015 (1984).
- <sup>12</sup>T. Matsushima and C. Adachi, *Thin Solid Films* **517**, 874 (2008).
- <sup>13</sup>C. S. Kim, S. Lee, L. L. Tinker, S. Bernhard, and Y. L. Loo, *Chem. Mater.* **21**, 4583 (2009).
- <sup>14</sup>M. F. Calhoun, J. Sanchez, D. Olaya, M. E. Gershenson, and V. Podzorov, *Nature Mater.* **7**, 84 (2008).
- <sup>15</sup>W. Zhao and A. Kahn, *J. Appl. Phys.* **105**, 123711 (2009).
- <sup>16</sup>A. Davison, R. H. Holm, R. E. Benson, and M. Mahler, *Inorg. Synth.* **10**, 8 (1967).
- <sup>17</sup>A. Wan, J. Hwang, F. Amy, and A. Kahn, *Org. Electron.* **6**, 47 (2005).
- <sup>18</sup>I. Salzmann, S. Duhm, R. Opitz, R. L. Johnson, J. P. Rabe, and N. Koch, *J. Appl. Phys.* **104**, 114518 (2008).
- <sup>19</sup>F. Amy, C. Chan, and A. Kahn, *Org. Electron.* **6**, 85 (2005).
- <sup>20</sup>M. Vissenberg and M. Matters, *Phys. Rev. B* **57**, 12964 (1998).
- <sup>21</sup>V. I. Adamovich, S. R. Cordero, P. I. Djurovich, A. Tamayo, M. E. Thompson, B. W. D'Andrade, and S. R. Forrest, *Org. Electron.* **4**, 77 (2003).
- <sup>22</sup>F. Dinelli, M. Murgia, P. Levy, M. Cavallini, F. Biscarini, and D. M. de Leeuw, *Phys. Rev. Lett.* **92**, 116802 (2004).
- <sup>23</sup>Y. Abe, T. Hasegawa, Y. Takahashi, T. Yamada, and Y. Tokura, *Appl. Phys. Lett.* **87**, 153506 (2005).